Inhibition of Cathepsin K Alleviates Autophagy-Related Inflammation in Periodontitis-Aggravating Arthritis

Yuan Yue,[a] Wuwei Yin,[b] Qin Yang,[a] Jie Ren,[a] Liangyu Tan,[a] Jiajia Wang,[a] Jie Liu,[a] Qiuyu Lu,[a] Handong Ding,[a] Weicheng Zhan,[a] Liang Hao,[a] Min Wang[a]

[a]The State Key Laboratory of Oral Diseases and National Clinical Research Center for Oral Diseases, Department of Prosthodontics, West China Hospital of Stomatology, Sichuan University, Sichuan, People's Republic of China
[b]Stomatological Hospital, Southern Medical University, Guangzhou, People's Republic of China

Yuan Yue and Wuwei Yin contributed equally to this work. Author order was determined by drawing straws.

ABSTRACT Rheumatoid arthritis (RA) and periodontitis share many epidemiological and pathological features, with emerging studies reporting a relationship between the two diseases. Recently, RA and periodontitis have been associated with autophagy. In the present study, we investigated the effects of cathepsin K (CtsK) inhibition on RA with periodontitis in a mouse model and its immunological function affecting autophagy. To topically inhibit CtsK periodontitis with arthritis in the animal model, adeno-associated virus (AAV) transfection was performed in periodontal and knee joint regions. Transfection of small interfering RNA (siRNA) was performed to inhibit CtsK in RAW264.7 cells. The effects of CtsK inhibition on the autophagy pathway were then evaluated in both *in vivo* and *in vitro* experiments. RA and periodontitis aggravated destruction and inflammation in their respective lesion areas. Inhibition of CtsK had multiple effects: (i) reduced destruction of alveolar bone and articular tissue, (ii) decreased macrophage numbers and inflammatory cytokine expression in the synovium, and (iii) alleviated expression of the autophagy-related transcription factor EB (TFEB) and microtubule-associated protein 1A/1B-light chain 3 (LC3) at the protein level in knee joints. Inhibition of CtsK *in vitro* reduced the expression of autophagy-related proteins and related inflammatory factors. Our data revealed that the inhibition of CtsK resisted the destruction of articular tissues and relieved inflammation from RA with periodontitis. Furthermore, CtsK was implicated as an imperative regulator of the autophagy pathway in RA and macrophages.

KEYWORDS periodontitis, collagen-induced arthritis, cathepsin K, autophagy

Inflammation and the immune response are inseparable. The development of chronic inflammatory diseases is closely related to the innate and adaptive immune systems. Rheumatoid arthritis (RA) is a chronic autoimmune disease, releasing chemicals that damage nearby bone, cartilage, tendons, and ligaments (1, 2). In addition to autoimmune disorders, a number of risk factors can trigger or exacerbate RA (3). For instance, periodontitis not only is a chronic inflammation that occurs in the oral cavity but also is a risk factor that may affect the progression of RA (4). In recent years, the relationships between RA and periodontitis have been extensively reviewed (5, 6). RA and periodontitis are both caused by immune disorders and are associated with inflammation and the destruction of soft tissue and bone. In addition, they share similar pathological mechanisms and the same genetic and environmental risk factors, such as smoking and obesity (7).

Autophagy is a normal physiological response to cell self-degradation. By regulating cell proliferation and cell death, autophagy also affects the immune response (8, 9). Not
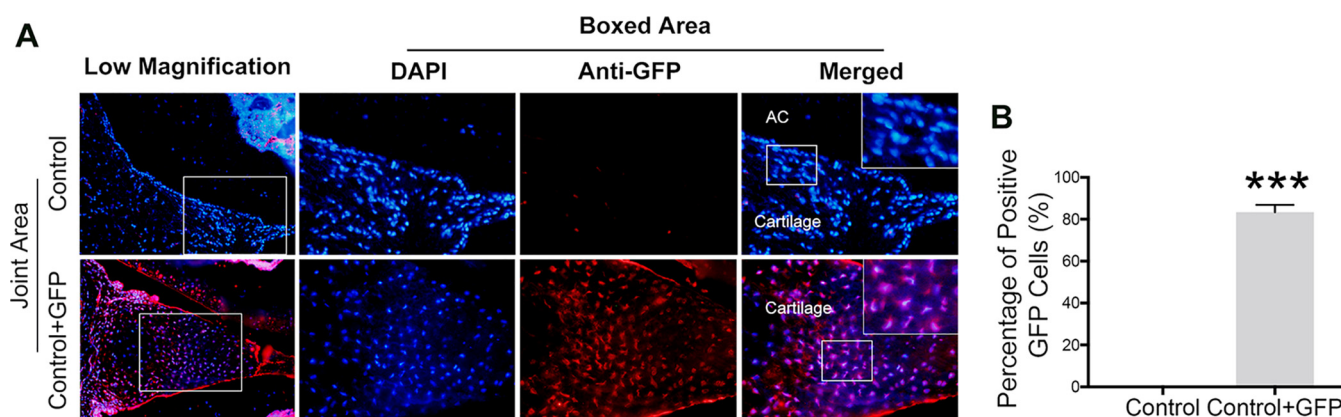
FIG 1 Immunofluorescence analysis of articular tissue in the control group and the empty AAV vector (GFP) group. (A) IF staining of GFP-positive cells in the articular area. Anti-mouse GFP antibody was applied to determine the AAV transfection efficiency. Red spots are GFP-positive cells. AC, articular cavity; DAPI, 4′,6-diamidino-2-phenylindole. (B) Quantification of GFP-positive cells. Control, untreated DBA/J1 mice; GFP, mice that received empty AAV vectors (AAV-U6-CAG-EGFP). Data are presented as means $\pm$ SD. Statistics were determined by a Mann-Whitney U exact test. The asterisk (with no line connection) on the column of this group represents the statistical difference between it and the control group. ***, $P < 0.001$.

surprisingly, autophagy disorders are involved in the pathogenesis of many diseases. For instance, a number of recent studies have shown a relationship between autophagy and RA (10–12) as well as between autophagy and periodontitis (13, 14). This gave us reason to speculate that autophagy may play an important role in RA and the exacerbation of RA by periodontitis.

Cathepsin K (CtsK) is lysosomal cysteine protease that is primarily expressed in osteoclasts and plays an important role in bone resorption (15). CtsK has been shown to be an effective therapeutic target for bone destruction-related diseases (16, 17). This has led to the function of CtsK inhibitors being evaluated in various animal models and preclinical studies. Unfortunately, the systemic administration of CtsK inhibitors and their nonselective nature result in adverse side effects and undesired drug-drug interactions (18). Our previous study revealed that the osteoimmunological function of CtsK regulates both periodontitis and RA through the Toll-like receptor 9 (TLR9) signaling pathway (19). Whereas TLR9 is closely related to autophagy (20, 21), it is likely that CtsK also affects the autophagy response in RA.

Adeno-associated viruses (AAVs) have become promising gene delivery vectors that provide a new and effective strategy to precisely target pathological genes and the tissues affected by some diseases (22). AAV-mediated gene therapy has been utilized in hundreds of animal experiments and clinical trials. It has been found to be safe and nonpathogenic in both animal and human hosts and causes only mild immune responses (23).

In the present study, we focused on the consequences of topical CtsK silencing through the localized administration of AAV-mediated RNA interference in a mouse model of RA and periodontitis. This was done to further explore the association between CtsK and autophagy *in vivo* and *in vitro*, which is important in order to determine whether CtsK might be a possible target to simultaneously treat both RA and periodontitis.

RESULTS

Localized inhibition of CtsK alleviates articular tissue destruction and paw swelling induced by CIA and reduces alveolar bone resorption in the periodontitis model. After ensuring that the AAVs had been successfully transfected into articular tissues (Fig. 1), we tested the expression of CTSK in the knee joint region. The immunohistochemistry (IHC) results showed that compared with the control group, both *Porphyromonas gingivalis* inoculation and collagen-induced arthritis (CIA) injection caused a significantly high expression level of CTSK in the knee joint region, and the expression level of CTSK was highest when the two interventions coexisted. AAV

transfection effectively inhibited the expression of CTSK in each group (see Fig. S1A and B in the supplemental material).

In order to further observe the lesion in the joint area, we carried out saffron O staining of the knee joint sections of each group. Saffron O staining analyses of knee joints revealed that the *Porphyromonas gingivalis* (*P.g*)+AAV(GFP) group, the CIA+AAV(GFP) group, and the CIA+*P.g*+AAV(GFP) group exhibit more severe cartilage damage and osteophyte formation than the control group. Localized inhibition of CtsK alleviated cartilage damage in the articular tissues (Fig. S2A). The histopathology assessment of osteoarthritis cartilage confirmed the data from saffron O staining analyses (Fig. S2B).

Heterologous type II collagen is widely used as an immunogen for the CIA model. In CIA-susceptible mice, the serum antibody levels to the type II collagen used for immunization are very high. Furthermore, these antibodies cross-react with various species of type II collagen, including autologous type II collagen, due to the conserved amino acid sequences of type II collagen. An enzyme-linked immunosorbent assay (ELISA) was used to detect the serum level of type II chicken collagen antibody in each group of mice, and it was found that the antibody level was higher in the CIA-induced arthritis group than in the control group and the *P.g*+AAV(GFP) group. There was no significant difference in antibody concentrations between the CIA+*P.g*+AAV(GFP) group and the CIA+AAV(GFP) group. Localized inhibition of CtsK significantly reduced the concentration of type II chicken collagen antibody in mouse serum (Fig. S3).

The development of arthritis in the CIA model is dependent upon the induction of anticollagen antibodies. We tested type I collagen by IHC to ensure that proper conclusions can be drawn. In the control group, the cartilage is not stained, while the subchondral bone is stained brown. In the *P.g*+AAV(GFP) group, IHC of type I collagen showed irregular staining in the superficial areas of the cartilage, and the staining was light brown. The fibrous tissue was stained positive and dark in the CIA+AAV(GFP) group. Compared with the CIA+AAV(GFP) group, the pigmentation area was dark and uneven and the fibrous tissue was irregularly curled in the CIA+*P.g*+AAV(GFP) group. Type I collagen was not expressed in normal cartilage, while type I collagen was highly expressed in cartilage when *P. gingivalis* inoculation and osteoarthritis coexisted. The localized inhibition of CtsK significantly reduced the expression of type I collagen in the articular tissues (Fig. S4).

We found that the localized inhibition of CtsK effectively relieved hind paw swelling (Fig. 2A) and delayed the initial onset of arthritis in mice transfected with AAV(CtsK) for 8 days (Fig. 2B). At the time of specimen collection, the incidence of arthritis in the CIA+AAV(GFP) transfection group was 90%, while the incidence of arthritis in the CIA+AAV(CtsK) transfection group was 70%. The incidence of arthritis was highest in the group with CIA with *P. gingivalis* inoculation and AAV(GFP) transfection (93.3%) but decreased to 85.7% in the group with CIA with *P. gingivalis* inoculation and AAV(CtsK) transfection after inhibition of CtsK (Fig. 2B). Inhibition of CtsK not only reduced the incidence of arthritis but also significantly reduced the average arthritis scores of the limbs (Fig. 2C), indicating that CtsK inhibition slowed the development of arthritis. In addition, the mice that received a *P. gingivalis* inoculation demonstrated a more acute onset of arthritis and more severe extremity swelling than those that did not receive *P. gingivalis*.

We quantitated the Cemento-Enamel Junction of the first molar to the Alveolar Bone Crest (CEJ-ABC) distances and analyzed vertical periodontal bone resorption based on the sagittal sectional images of the alveolar bones. The data showed that the CEJ-ABC distance for the comorbidity group was greater than that of the simple periodontitis group (Fig. 2D and E). Oral transfection of AAV(CtsK) reversed alveolar bone resorption in these two groups, with no significant difference being found among other groups. In addition to the data described above, we also found that periodontitis promoted the occurrence and development of arthritis and that arthritis also aggravated bone destruction in periodontitis disease. However, inhibiting CtsK effectively reduced the
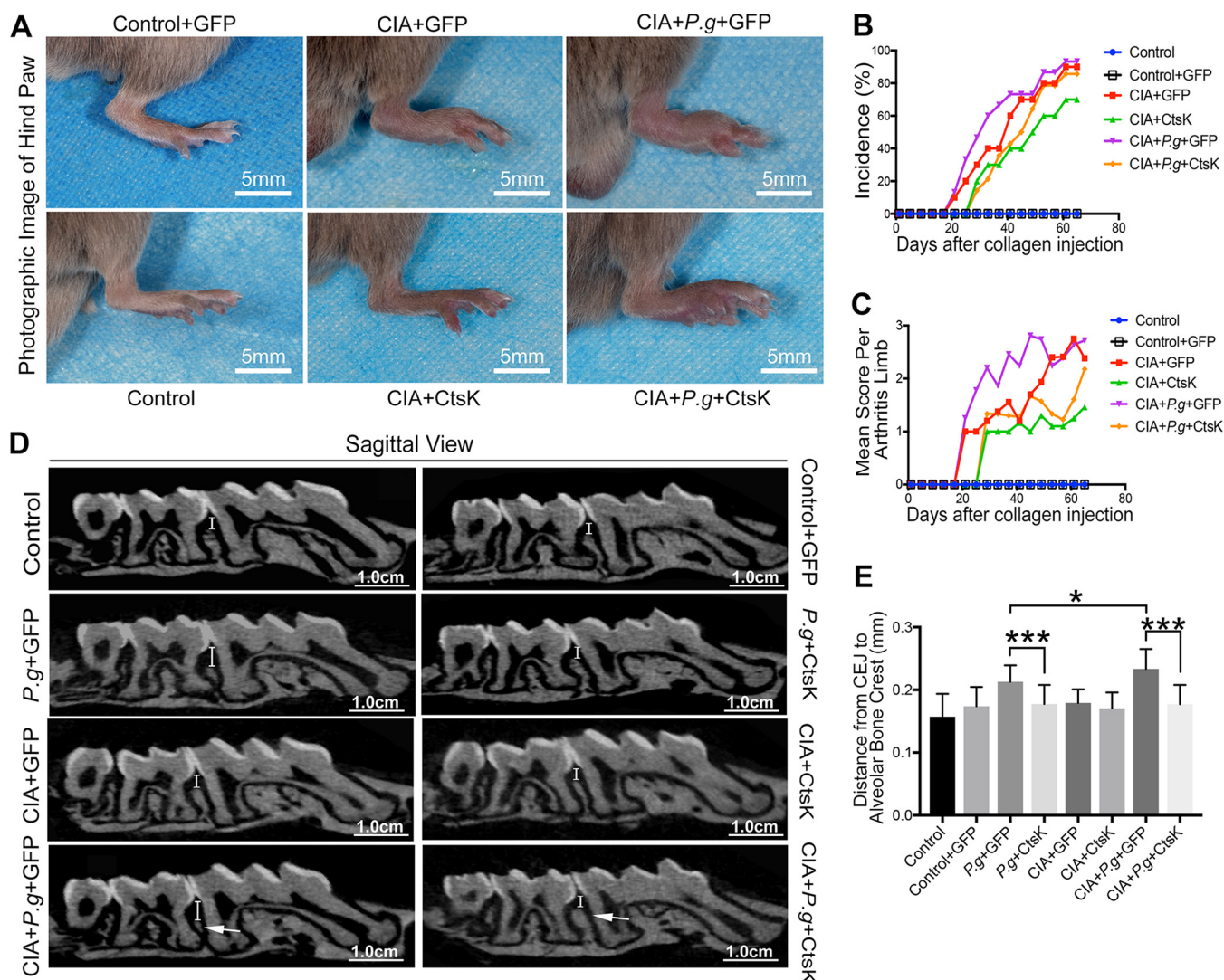
FIG 2 Localized inhibition of CtsK alleviates the swelling of paws induced by CIA and reduces bone destruction of alveolar bone. (A) Photographs of hind paws in different groups. (B) Incidences of CIA in different groups. (C) Mean scores per arthritic limb in different groups. (D) Sagittal view of alveolar bones scanned by micro-CT. (E) Distance from the cementoenamel junction of the first molar to the alveolar bone crest. Control, untreated DBA/J1 mice; *P.g*, mice orally infected with *Porphyromonas gingivalis*; CIA, mice with collagen-induced arthritis; GFP, mice that received empty AAV vectors (AAV-U6-CAG-EGFP); CtsK, mice that received AAV-U6-CtsK-shRNA-CAG-EGFP. Data are presented as means ± SD. Statistics in panel E were determined by ordinary one-way analysis of variance (ANOVA) and Student's *t* test. The asterisk (with no line connection) on the column of this group represents the statistical difference between it and the control group. *, $P < 0.05$; **, $P < 0.01$; ***, $P < 0.001$. Experiments were repeated three times.

damage in the lesion areas of both diseases, suggesting that CtsK was closely associated with arthritis and periodontitis-aggravating arthritis.

Localized inhibition of CtsK reduces the number of macrophages and the expression of inflammatory cytokines in the synovium. F4/80 is a specific marker of macrophages. The distribution of CTSK and F4/80 *in vivo* was detected by immunofluorescence (IF) colocation staining (Fig. S5). The IF results showed that *in vivo*, macrophages could express CTSK, so we determined the distribution of macrophages in the synovium. The immunohistochemical staining results showed that in the joint capsule area of knee joints, the number of F4/80-positive cells was significantly higher in the CIA+AAV(GFP) group and the CIA+*P.g*+AAV(GFP) group than in the CIA+AAV(CtsK) group and the CIA+*P.g*+AAV(CtsK) group. More interestingly, macrophages were primarily found in areas with damaged joint tissue. After the inhibition of CtsK, the number of macrophages in the same areas of each group was decreased to various degrees (Fig. 3A and B).
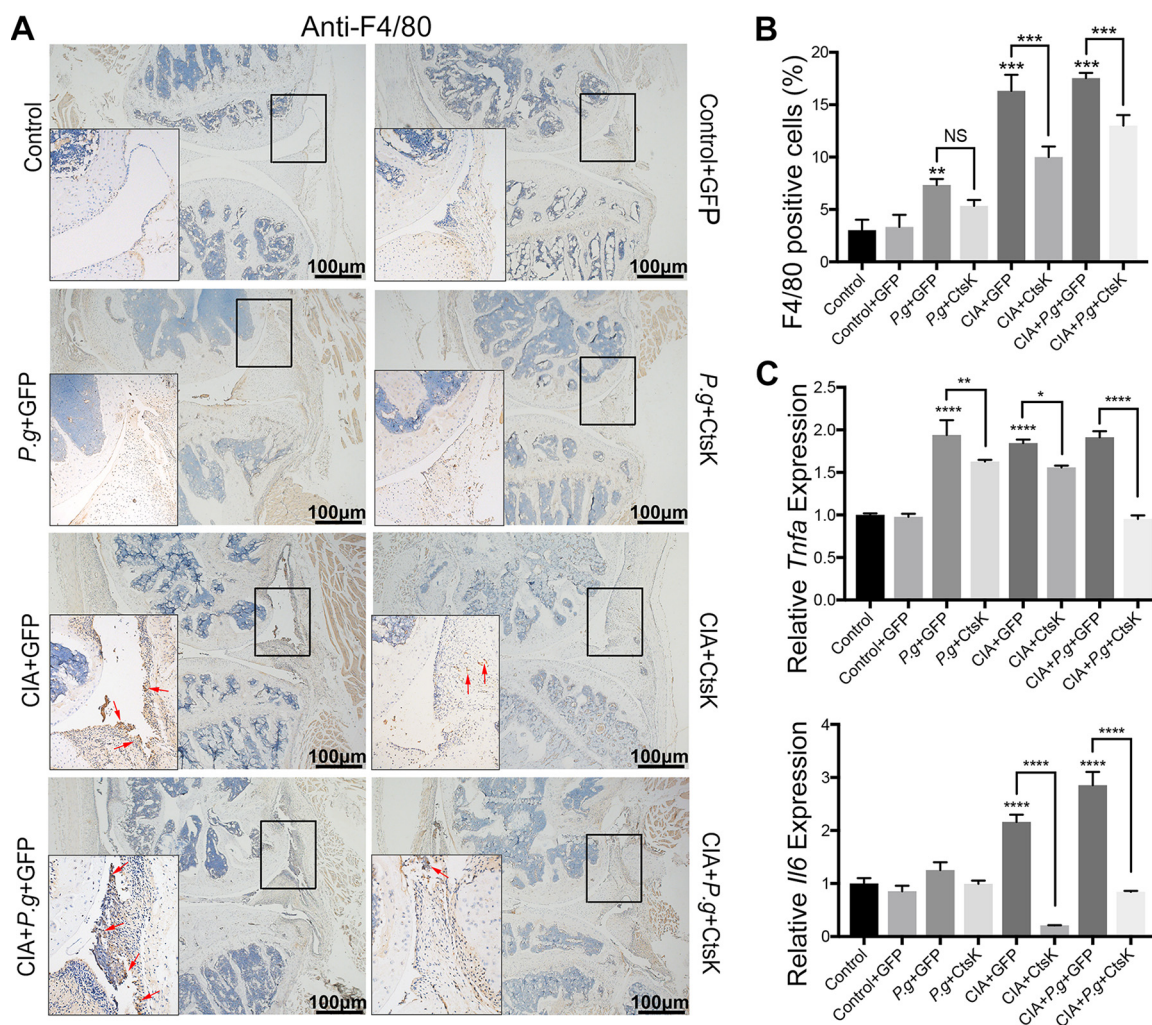
FIG 3 Localized inhibition of CtsK reduces the number of macrophages and the expression of inflammatory cytokines in the articular tissue. (A) IHC staining of F4/80-positive cells in the articular tissue. The red arrow indicates positive cells. (B) Quantification of F4/80-positive cells in panel A. (C) Relative mRNA expression levels of *Tnfα* and *Il6* in the articular tissue detected by qRT-PCR. Control, untreated DBA/J1 mice; *P.g*, mice orally infected with *Porphyromonas gingivalis*; CIA, mice with collagen-induced arthritis; GFP, mice that received empty AAV vectors (AAV-U6-CAG-EGFP); CtsK, mice that received AAV-U6-CtsK-shRNA-CAG-EGFP. Data are presented as means ± SD. Statistics in panel B were determined by a Kruskal-Wallis test and a Mann-Whitney U exact test. Statistics in panel C were determined by ordinary one-way ANOVA and Student's *t* test. The asterisk (with no line connection) on the column of this group represents the statistical difference between it and the control group. *, $P < 0.05$; **, $P < 0.01$; ***, $P < 0.001$; ****, $P < 0.0001$; NS, not significant. Experiments were repeated three times.

The relative mRNA expression levels of *Tnfα* and *Il6* in the knee joints of each group are shown in Fig. 3C. CIA increased the expression of *Tnfα* and *Il6* in the knee joints, with the CIA+*P.g*+AAV(GFP) group demonstrating the highest expression levels of *Tnfα* and *Il6* compared to those in the other groups. Interestingly, the elevated levels of *Tnfα* and *Il6* expression in the articular region declined in response to AAV(CtsK) transfection. Periodontitis induced greater numbers of macrophages and increased expression levels of inflammatory cytokines in the arthritis lesion areas, while the inhibition of CtsK significantly reduced the inflammatory immune response, suggesting that CtsK was associated with macrophages and inflammatory cytokines involved in the developmental process of arthritis and periodontitis-aggravating arthritis.

Localized inhibition of CtsK reduces autophagy-related protein expression in the synovium. To further explore the role of CtsK in the development of arthritis, we investigated the relationship between CtsK and autophagy in RA. Immunohistochemical results demonstrated that transcription factor EB (TFEB) protein expression was upregulated in the joint areas of the CIA+AAV(GFP) group and the CIA+*P.g*+AAV(GFP)

group, with the highest level of TFEB expression being observed in the CIA+*P.g*+AAV(GFP) group. Associated with the inhibition of CtsK in each group, TFEB expression decreased along with a reduction in the arthritis lesions (Fig. 4A and B). The data from reverse transcription-quantitative PCR (qRT-PCR) analysis of the joint tissues of each group confirmed the immunohistochemistry results (Fig. 4C).

In addition, we detected changes in CtsK and the autophagy pathway in joint tissue by Western blotting and qRT-PCR. We found that periodontitis promoted the expression of CtsK in the arthritis lesions, and at the same time, the expression levels of the autophagy proteins TFEB and light chain 3 (LC3) were upregulated (Fig. 5A). After effectively inhibiting the expression of CtsK, the expression levels of TFEB and LC3 were also decreased. The qRT-PCR results also showed that the changing trend of the autophagy pathway was similar to that of CtsK. Periodontitis promoted the upregulation of both *Tfeb* and *Lc3* in the arthritis lesions, with autophagy being downregulated by CtsK inhibition (Fig. 5B).

Inhibition of CtsK reduces the autophagy pathway in macrophages. To further explore the role of CtsK in macrophages, we chose the murine macrophage cell line RAW264.7 for use in our *in vitro* experiments. As a first step, 6-carboxy-fluorescein (FAM)-small interfering RNA (siRNA) was used to determine the transfection efficiency of the cells. Based on observations of the cells under an inverted fluorescence phase-contrast microscope, green fluorescence was scattered in the cytoplasm (Fig. 6A). CtsK expression was detected by Western blotting, which verified that siRNA treatment effectively inhibited the expression of CtsK at the protein level (Fig. 6B). In macrophages, the expressions of TFEB and LC3 were also downregulated after the inhibition of CtsK. These *in vitro* findings were consistent was the *in vivo* results (Fig. 6B). When the expression of CtsK was inhibited, the expression levels of *Il6* and *Tnfα* were significantly decreased (Fig. 6C).

DISCUSSION

The immune and bone systems communicate with each other through a plethora of transcription factors, cytokines, receptors, and signaling pathways. The interactions between these systems involve physiological processes regulating bone metabolism and may be more frequent in some autoimmune or inflammatory diseases (24). For instance, activated osteoclasts attached to bone surfaces are able to create acidic environments through proton pumps, which promotes the demineralization of bone tissue, and at the same time secrete matrix metalloproteinases and CtsK to directly degrade the organic bone matrix (25). Based on results from the present study, it is predicted that bone resorption in periodontal and knee joint areas will decrease once CtsK expression is suppressed. The *in vivo* results showed that RA and periodontitis were able to promote the progression of one another in a comorbid fashion, leading to more serious destruction than that caused by either condition individually.

As important cells of the innate immune system, macrophages are resident cells of synovial tissue. Studies have found that there are more M1 macrophages in the synovium of RA patients than in healthy people (26). Increased activation of macrophages is conducive to a vicious cycle of tissue damage. Macrophages can ultimately lead to joint destruction in individuals with RA by stimulating angiogenesis and inducing leukocyte and lymphocyte infiltration, fibroblast proliferation, and the secretion of tumor necrosis factor alpha (TNF-α), interleukin-1 (IL-1), IL-6, and matrix metalloproteinase (27, 28). Our present study found that destruction in articular lesions was significantly reduced after AAV(CtsK) transfection in the CIA and two-comorbidity groups. Furthermore, immunohistochemical staining revealed that the number of macrophages in inflamed areas also decreased following AAV(CtsK) transfection. These data suggested that CtsK might affect the body's immune response and inflammation by affecting the differentiation and activation of macrophages. Although CtsK inhibition was limited to periodontal and knee joint regions in this study, the arthritis scores of the hind paws of the mice suggested that the systemic inflammatory response of
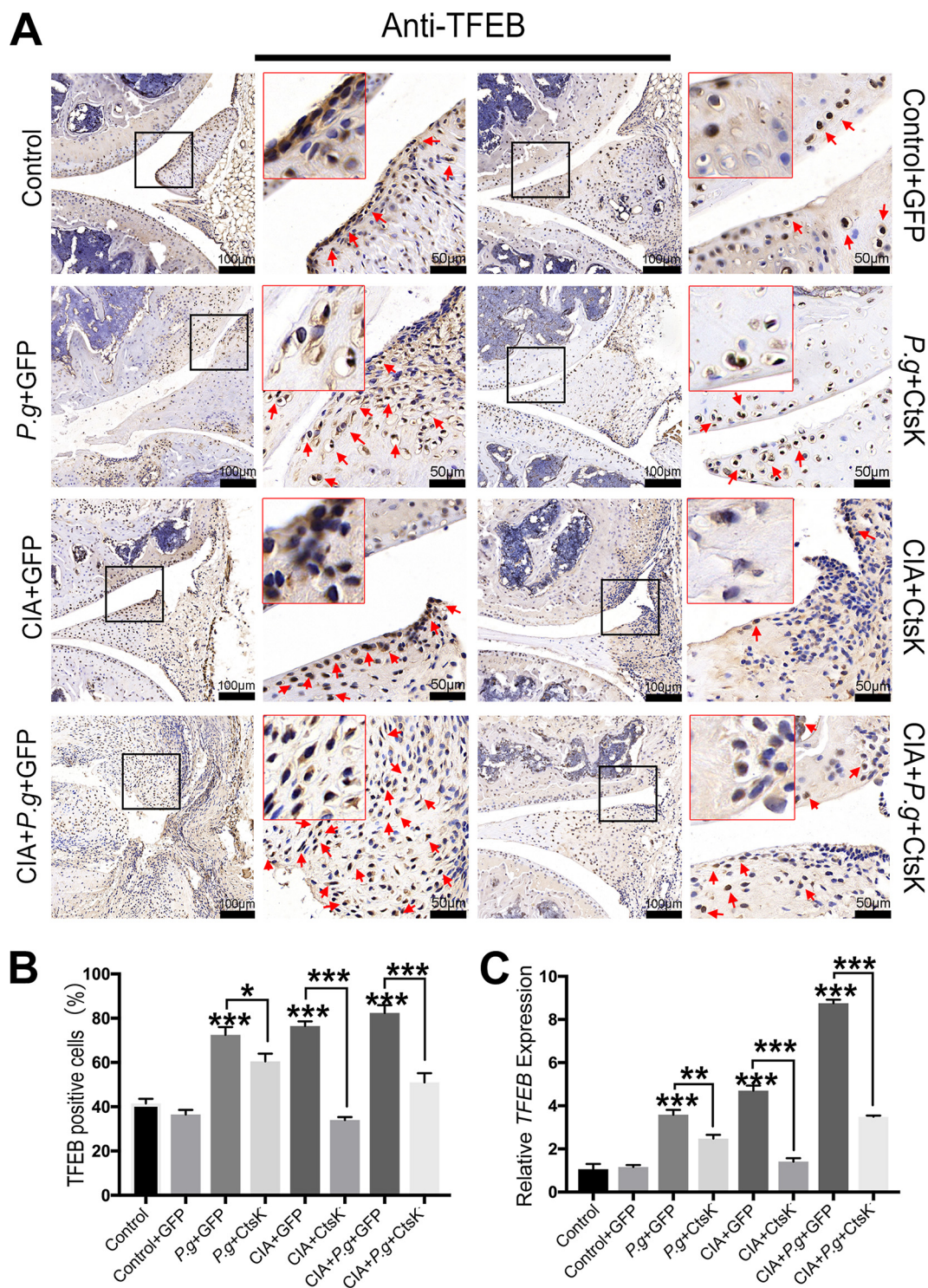
FIG 4 Inhibition of CtsK in the lesion area reduces the expression of TFEB in the articular tissue. (A) IHC staining of TFEB-positive cells in the articular tissue. The red arrows indicate positive cells. (B) Quantification of TFEB-positive cells in panel A. (C) Relative mRNA expression of *Tfeb* in articular lesions determined by qRT-PCR. Control, untreated DBA/J1 mice; *P.g*, mice orally infected with *Porphyromonas gingivalis*; CIA, mice with collagen-induced arthritis; GFP, mice that received empty AAV vectors (AAV-U6-CAG-EGFP); CtsK, mice that received AAV-U6-CtsK-shRNA-CAG-EGFP. Data are presented as means ± SD. Statistics in panel B were determined by a Kruskal-Wallis test and a Mann-Whitney U exact test. Statistics in panel C were determined by ordinary one-way ANOVA and Student's *t* test. The asterisk (with no line connection) on the column of this group represents the statistical difference between it and the control group. *, $P < 0.05$; **, $P < 0.01$; ***, $P < 0.001$. Experiments were repeated three times.

FIG 5 Inhibition of CtsK reduces the expression of the autophagy signaling pathway. (A) Western blotting of TFEB, CTSK, and LC3A/B in different groups. Representative images and normalized quantifications are shown. (B) Analysis by qRT-PCR of mRNA expression levels of *CtsK*, *Lc3*, and *P62* in the articular tissue. Control, untreated DBA/J1 mice; *P.g*, DBA/J1 mice orally infected with *Porphyromonas gingivalis*; CIA, mice with collagen-induced arthritis; GFP, mice that received empty AAV vectors (AAV-U6-CAG-EGFP); CtsK, mice that received AAV-U6-CtsK-shRNA-CAG-EGFP. Data are presented as means ± SD. Statistics in panels A and B were determined by ordinary one-way ANOVA and Student's *t* test. The asterisk (with no line connection) on the column of this group represents the statistical difference between it and the control group. *, $P < 0.05$; **, $P < 0.01$; ***, $P < 0.001$. Experiments were repeated three times.
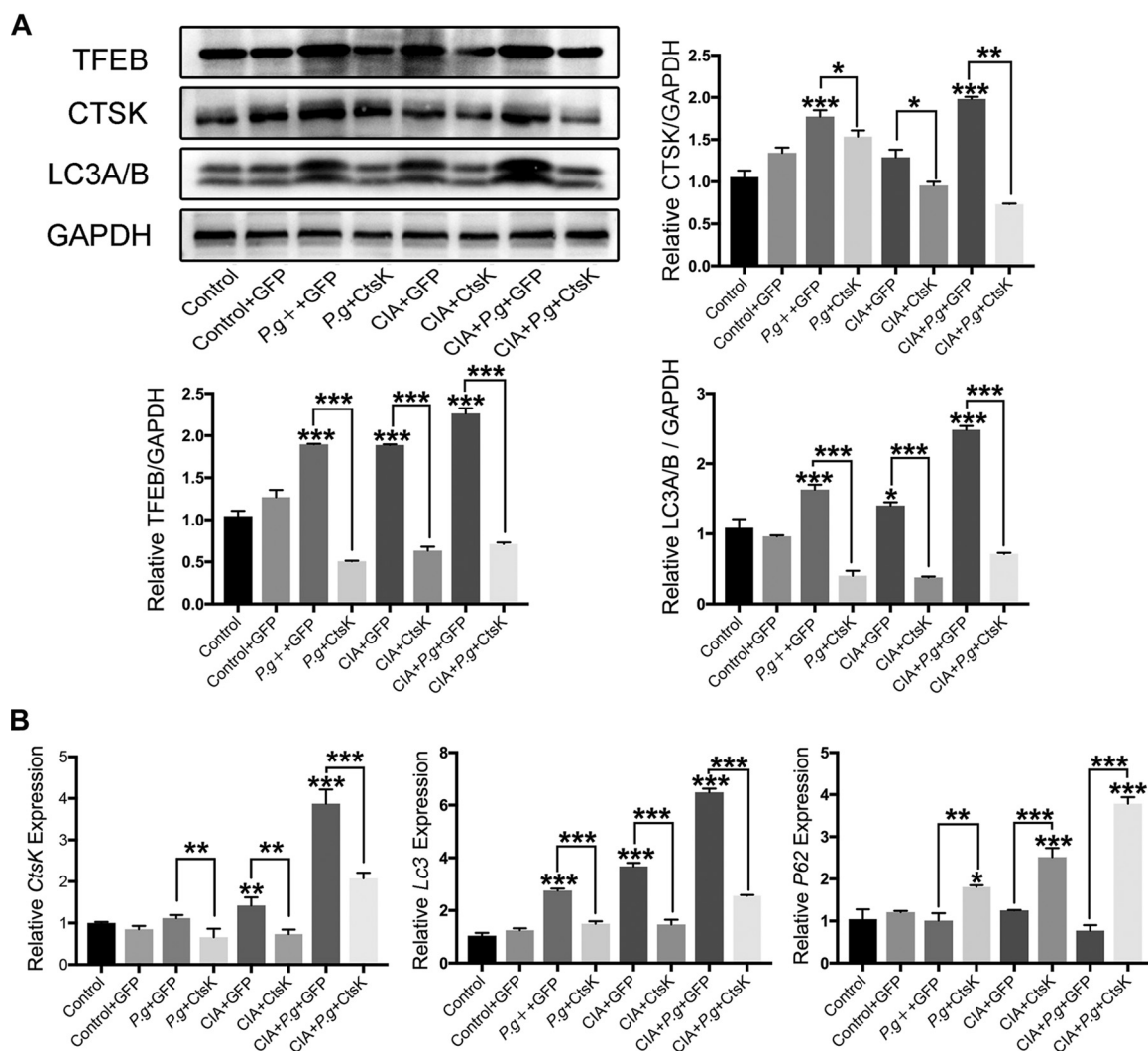
arthritis was alleviated, which may have been related to reduced macrophage activation and, subsequently, a decreased immune response throughout the body.

The relationship between arthritis and autophagy has been studied previously, and a large amount of the literature shows that autophagy is significantly enhanced during the course of arthritis (29–31). As the key protein in autophagy, TFEB activity is closely related to lysosome synthesis, autophagy, and the production of inflammatory cytokines. The overexpression of TFEB can lead to the activation of the autophagy pathway (32). Interestingly, we found not only that periodontitis increased TFEB expression in arthritic lesions but also that the expression of the TFEB protein was downregulated with the inhibition of CtsK *in vivo*. As we expected, the trend of other autophagy-related proteins, such as LC3, was similar to that of TFEB. The results from the cell culture experiments validated the conclusions made from the *in vivo* experiments. In the developmental processes of arthritis and periodontitis-aggravating arthritis, CtsK affected autophagy and inflammation.

Our previous study showed that CtsK is closely related to TLR9 in the development
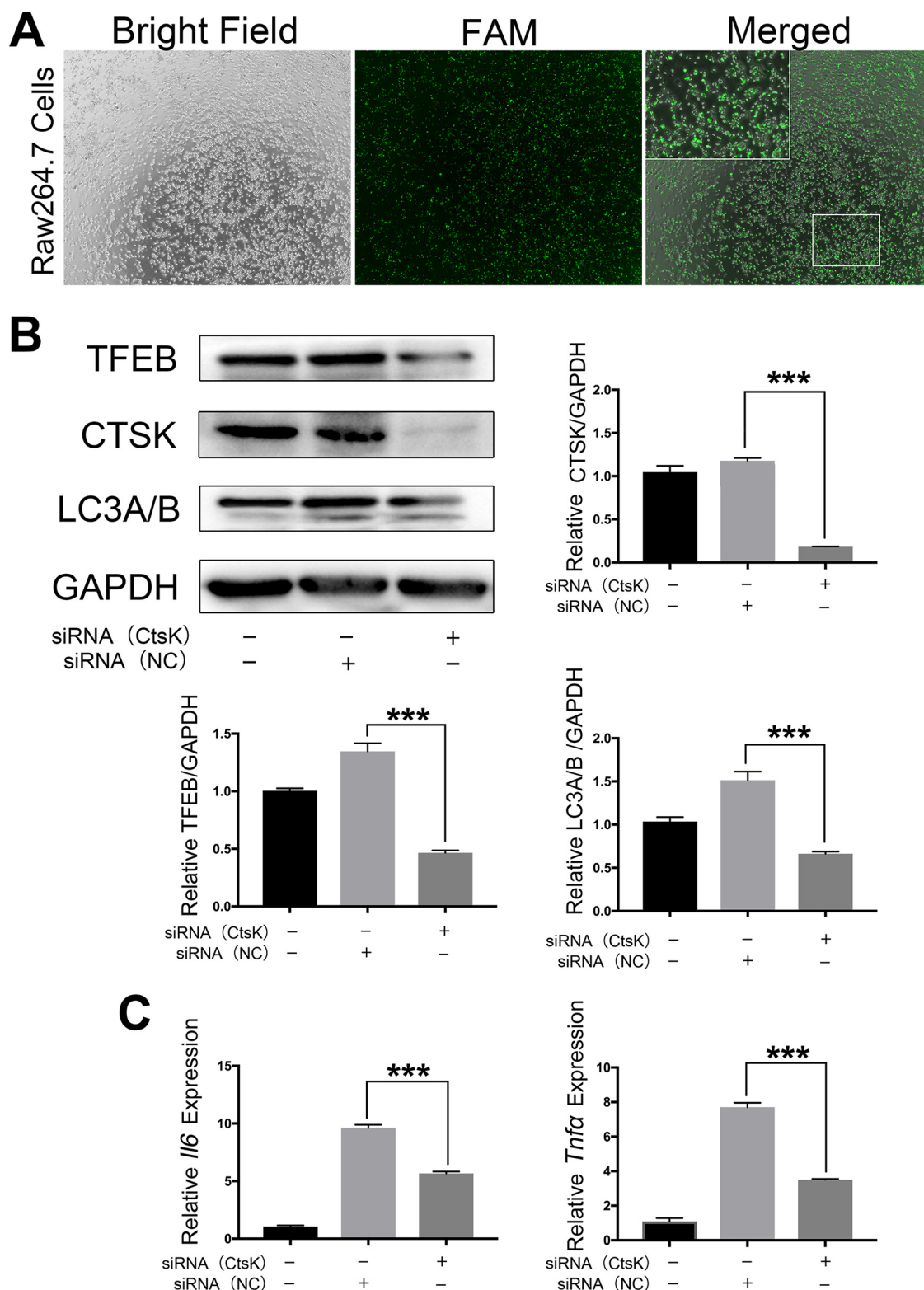
FIG 6 Inhibition of CtsK reduces the autophagy pathway in macrophages. (A) RAW264.7 cells were transfected with FAM-siRNA and observed under an inverted fluorescence microscope. Cells expressing green fluorescence were transfected successfully. (B) The expression of TFEB, CtsK, and LC3A/B at the protein level was determined by Western blotting. (C) The expression of *Il6* and *Tnfα* at the mRNA level was determined by qRT-PCR. Data are presented as means ± SD. Statistics in panels B and C were determined by ordinary one-way ANOVA and Student's *t* test. The asterisk (with no line connection) on the column of this group represents the statistical difference between it and the control group. ***, $P < 0.001$. Experiments were repeated three times. NC, nontargeting control.

of arthritis and periodontitis-aggravating arthritis (19). At the same time, a relationship between TLR9 and autophagy has also been demonstrated (21, 33, 34). Sanjuan et al. revealed that stimulating RAW264.7 cells with a TLR9 ligand promotes the maturation of phagosomes, which then participate in autophagy (35). These findings combined with the results from the present study suggest that in addition to the inhibition of the TLR9 signaling pathway, the reduction of TFEB expression may also contribute to the anti-inflammatory effects of CtsK inhibition. However, the mechanism of the interaction between CtsK, the TLR9 signaling pathway, autophagy, and inflammation requires further investigation.

A variety of pathogenic bacteria of periodontitis have been found to be associated with the onset or aggravation of RA (36, 37). *P. gingivalis* is the only bacterium known to secrete peptidylarginine deiminase (PAD enzyme), which can catalyze the citrullination of proteins and plays an important role in the occurrence of arthritis. Studies showed that in patients with rheumatoid arthritis and periodontitis, autoantibodies against citrulline histamine H3 could be produced in the body (38). *P. gingivalis* could promote the expression of citrulline antibody in the synovium of the joints of arthritic mice, which aggravated joint inflammation (39). Six periodontal pathogens could be detected in the synovial fluid of rheumatoid arthritis patients (40). The above-mentioned studies have proven that the pathogenesis and prognosis of RA may be closely related to oral microorganisms. However, whether oral microorganisms are related to the incidence of RA or whether they can become a biological indicator for RA detection is unknown, which is very worthy of discussion and research. Both RA and periodontitis cause chronic destruction of connective tissue and bone tissue caused by an imbalance of inflammation in the body. Therefore, we focused on the relationship between local diseases and systemic immune imbalance. This study revealed that localized inhibition of CtsK through AAV transfection was able to effectively reduce destruction in alveolar bone and articular areas, reduce the level of systemic inflammation in arthritis, decrease the number of macrophages in knee inflammation, and decrease the expression of autophagy-related proteins. We preliminarily explored the mechanism of CtsK affecting the autophagy pathway in RA and macrophages. Our data will provide a reference for other related studies of chronic diseases involving an imbalance in immune responses and bone destruction and serve as a basis to further explore the dual roles of CtsK as an osteoimmune gene in the immune and skeletal systems. Tissue-specific gene therapy targeting CtsK might be a promising direction in the treatment of rheumatoid arthritis and in future research.

MATERIALS AND METHODS

Animals. A total of 80 8-week-old male DBA/J1 mice (Chengdu Dashuo Experimental Animal Co. Ltd., China) were randomly assigned to eight groups: (i) control mice, which did not receive any treatment ($n = 5$); (ii) control+GFP mice, which were transfected with AAV expressing green fluorescent protein [AAV(GFP)] ($n = 5$); (iii) P.g+CtsK mice, which were transfected with AAV expressing CtsK and then orally infected with *Porphyromonas gingivalis* ($n = 10$); (iv) P.g+GFP mice, which were transfected with AAV(GFP) and then orally infected with *P. gingivalis* ($n = 10$); (v) CIA+CtsK mice, which were transfected with AAV(CtsK) and developed collagen-induced arthritis (CIA) ($n = 10$); (vi) CIA+GFP mice, which were transfected with AAV(GFP) and developed CIA ($n = 10$); (vii) CIA+P.g+CtsK mice, which were transfected with AAV(CtsK), developed CIA, and were orally infected with *P. gingivalis* ($n = 15$); and (viii) CIA+P.g+GFP mice, which were transfected with AAV(GFP), developed CIA, and were orally infected with *P. gingivalis* ($n = 15$). The study was approved by the Sichuan University Institutional Animal Care and Use Committee (protocol number WCCSIRB-D-2015-030). All animals were raised at the State Key Laboratory for Oral Disease animal facilities (Sichuan University, Sichuan, People's Republic of China), which are for specific-pathogen-free animals.

Experimental periodontitis and collagen-induced arthritis. The periodontitis and CIA mouse models were established according to our previously described protocols (19, 41, 42). For the periodontitis mouse model, we chose *P. gingivalis* (ATCC 33277) from the American Type Culture Collection to induce oral infection in the mice. To remove other potential pathogens from the mice during the washout period, kanamycin was added to the drinking water at a concentration of 0.5 mg/ml for 3 days prior to formal oral bacteria colonization. The bacteria and 3% sterile carboxymethyl cellulose (CMC) were evenly mixed into a gel state with a final concentration of *P. gingivalis* bacteria of 5×10^{10} cells/ml. The mixture containing bacteria was applied to the oral cavity of the mice for eight consecutive days using cotton swabs. For the CIA mouse model, chicken type II collagen was emulsified in 100 μg complete Freund's adjuvant. The emulsion was then slowly injected in 50 μl into the tissue between the mouse tail

veins. Fourteen days after the first infusion, the treatment was repeated to enhance the immune response. After the first injection of collagen, a daily score was recorded based on previously described protocols (43, 44).

AAV transfection. AAVs were purchased from Genechem Co. (Shanghai, China). As a negative control, empty AAVs were used. The AAVs were diluted with phosphate-buffered saline (PBS) to a final working concentration of 2.5×10^{10} g/ml (45). Using 100-μl microsyringes, 10 μl of an AAV working solution was injected into each knee and the buccal and palatal periodontal regions. After mice were injected with chicken type II collagen, AAV transfection was carried out once every 3 days. A total of eight AAV transfections were performed during the experimental period (17).

Tissue samples. There was no adverse event in each experimental group. A total of 80 mice were euthanized with an overdose of 10% chloral hydrate after a 65-day-postimmunization booster. Bilateral alveolar bones and the treated knee joints were collected. After being fixed in 4% paraformaldehyde, the specimens were subjected to micro-computed tomography (micro-CT) and histological analysis. The articular specimens used for RNA extraction were immersed in RNAlater, and the articular specimens used for protein extraction were stored at −80°C. Mouse serum was collected and stored at −80°C for subsequent ELISAs.

Micro-CT scanning. Maxilla samples were evaluated by micro-CT scanning using a vivaCT80 scanner (Scanco Medical, Switzerland). Scanning conditions were as follows: a source voltage of 70 kV, a source current of 114 μA, an exposure time of 200 ms, and a resolution of alveolar bone of 12 μm. Meanwhile, vertical alveolar bone resorption was evaluated by measuring the distance from the first-molar enamel-cement interface (CEJ) to the alveolar bone crest (ABC) (46).

Immunohistochemistry and immunofluorescence analyses. Paraffin-embedded specimens analyzed by immunohistochemistry (IHC) or immunofluorescence (IF) were sectioned at a thickness of 5 μm. After blocked with serum, the sections were treated with rabbit monoclonal antibodies against GFP (catalog number 2956; Cell Signaling Technology, USA), F4/80 (catalog number 70076; Cell Signaling Technology, USA), F4/80 (catalog number 30325; Cell Signaling Technology, USA), and transcription factor EB (TFEB) (catalog number A303-673A; Bethyl Laboratories, USA); cathepsin K (CTSK) polyclonal antibody (catalog number PA5-109605; Thermo Fisher, USA); or collagen I polyclonal antibody (catalog number PA1-26204; Thermo Fisher, USA) as primary antibodies, according to the manufacturers' instructions. The next day, the sections were incubated with the secondary antibody. CTSK is a cytoplasmic protein, and the brownish-stained cytoplasmic cells in the tissue sections were the positive cells. TFEB entered the nucleus and played a role, so the brownish-stained cells in the tissue section were the positive cells. F4/80 is a membrane protein, and the brown-stained cells in the tissue sections were the positive cells. Collagen type I was a component of the extracellular matrix, and the positive extracellular matrix in the tissue section was tan. The slices in the sagittal direction were numbered from the first section, where the femoral joint head, tibial joint head, and joint capsule appeared at the same time, to the end, where they started to disappear. The sample slice numbers of each group for the staining experiments were the same. For IHC and IF quantitative analyses, there were three sections in each group. To avoid artificially selecting the field of interest and affecting the statistical results, we randomly selected a high-magnification field in the knee joint. After selecting the region of interest, counts for each group were performed within the same region of interest. Positive cell and total cell counts were performed for each field, and the proportion of positive cells was calculated. Finally, the proportions of positive cells in each group were compared.

Saffron O staining. Paraffin-embedded specimens analyzed by saffron O staining were sectioned at a thickness of 5 μm according to the instructions of the kit (catalog number G2540; Solarbio, China). The sections were soaked in freshly prepared Weigert solution for 3 to 5 min, treated with an acidic ethanol solution for 15 s, washed with distilled water for 10 min, and soaked in a safranin O solution for 1 to 2 min. The Osteoarthritis Research Society International (OARSI) osteoarthritis cartilage histopathology assessment system was used to score each group of knee sections, as follows: grade 0 for intact surface and intact cartilage morphology; grade 1 for intact surface, superficial fibrillation, and edema, cell death, or cell proliferation; grade 2 for surface discontinuity; grade 3 for vertical fissures (clefts); grade 4 for erosion; and grade 5 for denudation. There were three sections in each group, and the scores for each group were quantitatively compared.

Mouse anti-type II collagen IgG assay kit with TMB. After the collection of mouse serum, an operation was carried out according to the instructions of the mouse anti-type I and -type II collagen IgG assay kit with tetramethylbenzidine (TMB) (catalog number 2031T; Chondrex, USA), and a spectrophotometer was used for detection.

Cell culture and small interfering RNA transfection. The murine macrophage cell line RAW264.7 was purchased from the ATCC. The cells were cultured in high-glucose Dulbecco's modified Eagle's medium (DMEM). The concentration of fetal bovine serum (FBS) in the culture medium was 10%. The cells were removed from the culture flasks using a cell scraper and prepared for seeding. The cell concentration was adjusted to approximately 2.5×10^5 cells/ml, and 2 ml of the cell suspension was seeded into T25 culture flasks. After the cells had adhered to the flask surface, an additional 2 ml of complete medium was added to each flask, and the cells were cultured. At 24 h postseeding, the cell density was confirmed to be approximately 30% to 50% confluent by microscopic examination, and small interfering RNA (siRNA) transfection was started. The CtsK-Mus-418 siRNA and negative-control siRNA were purchased from GenePharma, China. According to the manufacturer's instructions, siRNA and EndoFectin-Max transfection reagent (GeneCopoeia, USA) were each diluted with Opti-MEM, mixed, and then incubated at room temperature for 25 min. Additional high-glucose DMEM was added so that the final concentration of siRNA was 100 nM. Four milliliters of the siRNA-reagent complexes was added

dropwise to the cells and carefully dispersed over the entire surface area of the culture plate. After incubation with the siRNA for 24 h, the cells were cultured with high-glucose DMEM–10% FBS without siRNA. The RNA and protein were harvested from the cells 24 h later.

Reverse transcription-quantitative PCR analysis. Total RNA was extracted from the *in vitro* and *in vivo* specimens using an RNApure total RNA kit (BioTeke, China). Reverse transcription of the total RNA into cDNA was performed using a RevertAid first-strand cDNA synthesis kit (Thermo, USA). Gene expression levels were evaluated using the following gene-specific PCR primers: *CtsK* forward primer CCAGGAAATGAGCTTGACAAA, *CtsK* reverse primer ATAATTCTCAGTCACACAGTCCACA, interleukin-6 (*Il6*) forward primer CTCTGCAAGAGACTTCCATCCAGT, *Il6* reverse primer GAAGTAGGGAAGGCCGTGG, tumor necrosis factor alpha (*Tnfα*) forward primer AGGGTCTGGGCCATAGAACT, *Tnfα* reverse primer CCACCAC GCTCTTCTGTCTAC, *Tfeb* forward primer CCACCCCAGCCATCAACAC, *Tfeb* reverse primer CAGACAGATAC TCCCGAACCTT, *Lc3* forward primer GACCGCTGTAAGGAGGTGC, *Lc3* reverse primer CTTGACCAACTCGCT CATGTTA, *P62* forward primer AGGATGGGGACTTGGTTGC, and *P62* reverse primer TCACAGATCACATTG GGGTGC. The expression of the glyceraldehyde-3-phosphate dehydrogenase (GAPDH) gene (*Gapdh*), analyzed by PCR using *Gapdh* forward primer AGGTTGTCTCCTGCGACTTCA and *Gapdh* reverse primer CCAGGAAATGAGCTTGACAAA, was used as an endogenous sample control.

Western blot analysis. Total proteins from the mouse joint samples and cultured cells were extracted using a total protein extraction kit (catalog number PE001; SAB, China). The concentration of total proteins was measured using a bicinchoninic acid (BCA) protein assay kit (catalog number P0012S; Beyotime, China). Protein samples were resolved by electrophoresis and then transferred onto membranes. After blocking with 5% bovine serum albumin (BSA), the membranes were blotted using specific antibodies and visualized using a ChemiDoc Touch chemiluminescence system (Bio-Rad, USA). The primary antibodies used were specific for TFEB, CTSK, LC3A/B, and GAPDH (catalog numbers 32361, 4980, 12741, and 5174, respectively; Cell Signaling Technology).

Statistical analysis. Data are shown as means $\pm$ standard deviations (SD) for the different groups. In Fig. 1B, the differences between two groups were analyzed by a nonparametric Mann-Whitney U exact test. In Fig. 3B, Fig. 4B, Fig. S1B, and Fig. S2B, the differences between multiple groups were analyzed by a Kruskal-Wallis test, and the differences between two groups were analyzed by a nonparametric Mann-Whitney U exact test. In Fig. 2E, Fig. 3C, Fig. 4C, Fig. 5A and B, Fig. 6B and C, and Fig. S3, any differences between multiple groups were analyzed by ordinary one-way analysis of variance (ANOVA), and the differences between two groups were analyzed by parametric Student's *t* test. Data analysis was done by using GraphPad Prism 7 software. P values of <0.05 or U values of >1.96 were considered statistically significant.

SUPPLEMENTAL MATERIAL

Supplemental material is available online only.

SUPPLEMENTAL FILE 1, PDF file, 4.9 MB.

SUPPLEMENTAL FILE 2, PDF file, 7.4 MB.

SUPPLEMENTAL FILE 3, PDF file, 0.1 MB.

SUPPLEMENTAL FILE 4, PDF file, 1.8 MB.

SUPPLEMENTAL FILE 5, PDF file, 1.3 MB.

ACKNOWLEDGMENTS

REFERENCES

1. Scott DL, Wolfe F, Huizinga TW. 2010. Rheumatoid arthritis. Lancet 376:1094–1108. https://doi.org/10.1016/S0140-6736(10)60826-4.
2. Lee DM, Weinblatt ME. 2001. Rheumatoid arthritis. Lancet 358:903–911. https://doi.org/10.1016/S0140-6736(01)06075-5.
3. Kahlenberg JM, Fox DA. 2011. Advances in the medical treatment of rheumatoid arthritis. Hand Clin 27:11–20. https://doi.org/10.1016/j.hcl.2010.09.002.
4. Hajishengallis G. 2015. Periodontitis: from microbial immune subversion to systemic inflammation. Nat Rev Immunol 15:30–44. https://doi.org/10.1038/nri3785.
5. Leech MT, Bartold PM. 2015. The association between rheumatoid arthritis and periodontitis. Best Pract Res Clin Rheumatol 29:189–201. https://doi.org/10.1016/j.berh.2015.03.001.
6. Cheng Z, Meade J, Mankia K, Emery P, Devine DA. 2017. Periodontal disease and periodontal bacteria as triggers for rheumatoid arthritis. Best Pract Res Clin Rheumatol 31:19–30. https://doi.org/10.1016/j.berh.2017.08.001.
7. Di Giuseppe D, Discacciati A, Orsini N, Wolk A. 2014. Cigarette smoking and risk of rheumatoid arthritis: a dose-response meta-analysis. Arthritis Res Ther 16:R61. https://doi.org/10.1186/ar4498.

8. Glick D, Barth S, Macleod KF. 2010. Autophagy: cellular and molecular mechanisms. J Pathol 221:3–12. https://doi.org/10.1002/path.2697.

9. Yin Z, Pascual C, Klionsky DJ. 2016. Autophagy: machinery and regulation. Microb Cell 3:588–596. https://doi.org/10.15698/mic2016.12.546.

10. Vomero M, Barbati C, Colasanti T, Perricone C, Novelli L, Ceccarelli F, Spinelli FR, Di Franco M, Conti F, Valesini G, Alessandri C. 2018. Autophagy and rheumatoid arthritis: current knowledges and future perspectives. Front Immunol 9:1577. https://doi.org/10.3389/fimmu.2018.01577.

11. Chen Y-M, Chang C-Y, Chen H-H, Hsieh C-W, Tang K-T, Yang M-C, Lan J-L, Chen D-Y. 2018. Association between autophagy and inflammation in patients with rheumatoid arthritis receiving biologic therapy. Arthritis Res Ther 20:268. https://doi.org/10.1186/s13075-018-1763-0.

12. Kato M, Ospelt C, Gay RE, Gay S, Klein K. 2014. Dual role of autophagy in stress-induced cell death in rheumatoid arthritis synovial fibroblasts. Arthritis Rheumatol 66:40–48. https://doi.org/10.1002/art.38190.

13. Liu C, Mo L, Niu Y, Li X, Zhou X, Xu X. 2017. The role of reactive oxygen species and autophagy in periodontitis and their potential linkage. Front Physiol 8:439. https://doi.org/10.3389/fphys.2017.00439.

14. Zhuang H, Ali K, Ardu S, Tredwin C, Hu B. 2016. Autophagy in dental tissues: a double-edged sword. Cell Death Dis 7:e2192. https://doi.org/10.1038/cddis.2016.103.

15. Novinec M, Lenarcic B. 2013. Cathepsin K: a unique collagenolytic cysteine peptidase. Biol Chem 394:1163–1179. https://doi.org/10.1515/hsz-2013-0134.

16. Han J, Wei L, Xu W, Lu J, Wang C, Bao Y, Jia W. 2015. CTSK inhibitor exert its anti-obesity effects through regulating adipocyte differentiation in high-fat diet induced obese mice. Endocr J 62:309–317. https://doi.org/10.1507/endocrj.EJ14-0336.

17. Chen W, Gao B, Hao L, Zhu G, Jules J, MacDougall MJ, Wang J, Han X, Zhou X, Li YP. 2016. The silencing of cathepsin K used in gene therapy for periodontal disease reveals the role of cathepsin K in chronic infection and inflammation. J Periodontal Res 51:647–660. https://doi.org/10.1111/jre.12345.

18. Costa AG, Cusano NE, Silva BC, Cremers S, Bilezikian JP. 2011. Cathepsin K: its skeletal actions and role as a therapeutic target in osteoporosis. Nat Rev Rheumatol 7:447–456. https://doi.org/10.1038/nrrheum.2011.77.

19. Pan W, Yin W, Yang L, Xue L, Ren J, Wei W, Lu Q, Ding H, Liu Z, Nabar NR, Wang M, Hao L. 2019. Inhibition of Ctsk alleviates periodontitis and comorbid rheumatoid arthritis via downregulation of the TLR9 signalling pathway. J Clin Periodontol 46:286–296. https://doi.org/10.1111/jcpe.13060.

20. Delgado MA, Deretic V. 2009. Toll-like receptors in control of immunological autophagy. Cell Death Differ 16:976–983. https://doi.org/10.1038/cdd.2009.40.

21. Lim JS, Kim HS, Nguyen KC, Cho KA. 2016. The role of TLR9 in stress-dependent autophagy formation. Biochem Biophys Res Commun 481:219–226. https://doi.org/10.1016/j.bbrc.2016.10.105.

22. Daya S, Berns KI. 2008. Gene therapy using adeno-associated virus vectors. Clin Microbiol Rev 21:583–593. https://doi.org/10.1128/CMR.00008-08.

23. Mingozzi F, High KA. 2011. Therapeutic in vivo gene transfer for genetic disease using AAV: progress and challenges. Nat Rev Genet 12:341–355. https://doi.org/10.1038/nrg2988.

24. Walsh MC, Takegahara N, Kim H, Choi Y. 2018. Updating osteoimmunology: regulation of bone cells by innate and adaptive immunity. Nat Rev Rheumatol 14:146–156. https://doi.org/10.1038/nrrheum.2017.213.

25. Bar-Shavit Z. 2007. The osteoclast: a multinucleated, hematopoietic-origin, bone-resorbing osteoimmune cell. J Cell Biochem 102:1130–1139. https://doi.org/10.1002/jcb.21553.

26. Ma YY, Pope RM. 2005. The role of macrophages in rheumatoid arthritis. Curr Pharm Des 11:569–580. https://doi.org/10.2174/1381612053381927.

27. Navegantes KC, Gomes RDS, Pereira PAT, Czaikoski PG, Azevedo CHM, Monteiro MC. 2017. Immune modulation of some autoimmune diseases: the critical role of macrophages and neutrophils in the innate and adaptive immunity. J Transl Med 15:36. https://doi.org/10.1186/s12967-017-1141-8.

28. Wynn TA, Chawla A, Pollard JW. 2013. Macrophage biology in development, homeostasis and disease. Nature 496:445–455. https://doi.org/10.1038/nature12034.

29. Li YS, Zhang FJ, Zeng C, Luo W, Xiao WF, Gao SG, Lei GH. 2016. Autophagy in osteoarthritis. Joint Bone Spine 83:143–148. https://doi.org/10.1016/j.jbspin.2015.06.009.

30. Luo P, Gao F, Niu D, Sun X, Song Q, Guo C, Liang Y, Sun W. 2019. The role of autophagy in chondrocyte metabolism and osteoarthritis: a comprehensive research review. Biomed Res Int 2019:5171602. https://doi.org/10.1155/2019/5171602.

31. Onuora S. 2012. Bone research: autophagy is central to joint destruction in arthritis. Nat Rev Rheumatol 8:633. https://doi.org/10.1038/nrrheum.2012.171.

32. Brady OA, Martina JA, Puertollano R. 2018. Emerging roles for TFEB in the immune response and inflammation. Autophagy 14:181–189. https://doi.org/10.1080/15548627.2017.1313943.

33. Shi CS, Kehrl JH. 2008. MyD88 and Trif target Beclin 1 to trigger autophagy in macrophages. J Biol Chem 283:33175–33182. https://doi.org/10.1074/jbc.M804478200.

34. Minton K. 2018. LC3 anchors TLR9 signalling. Nat Rev Immunol 18:418–419. https://doi.org/10.1038/s41577-018-0019-1.

35. Sanjuan MA, Dillon CP, Tait SWG, Moshiach S, Dorsey F, Connell S, Komatsu M, Tanaka K, Cleveland JL, Withoff S, Green DR. 2007. Toll-like receptor signalling in macrophages links the autophagy pathway to phagocytosis. Nature 450:1253–1257. https://doi.org/10.1038/nature06421.

36. Steffen U, Schett G, Bozec A. 2019. How autoantibodies regulate osteoclast induced bone loss in rheumatoid arthritis. Front Immunol 10:1483. https://doi.org/10.3389/fimmu.2019.01483.

37. Nesse W, Westra J, van der Wal JE, Abbas F, Nicholas AP, Vissink A, Brouwer E. 2012. The periodontium of periodontitis patients contains citrullinated proteins which may play a role in ACPA (anti-citrullinated protein antibody) formation. J Clin Periodontol 39:599–607. https://doi.org/10.1111/j.1600-051X.2012.01885.x.

38. Janssen KMJ, de Smit MJ, Withaar C, Brouwer E, van Winkelhoff AJ, Vissink A, Westra J. 2017. Autoantibodies against citrullinated histone H3 in rheumatoid arthritis and periodontitis patients. J Clin Periodontol 44:577–584. https://doi.org/10.1111/jcpe.12727.

39. Jeong SH, Nam Y, Jung H, Kim J, Rim YA, Park N, Lee K, Choi S, Jang Y, Kim Y, Moon JH, Jung SM, Park SH, Ju JH. 2018. Interrupting oral infection of Porphyromonas gingivalis with anti-FimA antibody attenuates bacterial dissemination to the arthritic joint and improves experimental arthritis. Exp Mol Med 50:e460. https://doi.org/10.1038/emm.2017.301.

40. Moen K, Brun JG, Valen M, Skartveit L, Eribe EK, Olsen I, Jonsson R. 2006. Synovial inflammation in active rheumatoid arthritis and psoriatic arthritis facilitates trapping of a variety of oral bacterial DNAs. Clin Exp Rheumatol 24:656–663. https://www.ncbi.nlm.nih.gov/pubmed/17207381.

41. Pan W, Yang L, Li J, Xue L, Wei W, Ding H, Deng S, Tian Y, Yue Y, Wang M, Hao L, Chen Q. 2019. Traumatic occlusion aggravates bone loss during periodontitis and activates Hippo-YAP pathway. J Clin Periodontol 46:438–447. https://doi.org/10.1111/jcpe.13065.

42. Wei W, Xiao X, Li J, Ding H, Pan W, Deng S, Yin W, Xue L, Lu Q, Yue Y, Tian Y, Wang M, Hao L. 2019. Activation of the STAT1 pathway accelerates periodontitis in Nos3(−/−) mice. J Dent Res 98:1027–1036. https://doi.org/10.1177/0022034519858063.

43. Inglis JJ, Simelyte E, McCann FE, Criado G, Williams RO. 2008. Protocol for the induction of arthritis in C57BL/6 mice. Nat Protoc 3:612–618. https://doi.org/10.1038/nprot.2008.19.

44. Brand DD, Latham KA, Rosloniec EF. 2007. Collagen-induced arthritis. Nat Protoc 2:1269–1275. https://doi.org/10.1038/nprot.2007.173.

45. Vassalli G, Bueler H, Dudler J, von Segesser LK, Kappenberger L. 2003. Adeno-associated virus (AAV) vectors achieve prolonged transgene expression in mouse myocardium and arteries in vivo: a comparative study with adenovirus vectors. Int J Cardiol 90:229–238. https://doi.org/10.1016/S0167-5273(02)00554-5.

46. Park CH, Abramson ZR, Taba M, Jr, Jin Q, Chang J, Kreider JM, Goldstein SA, Giannobile WV. 2007. Three-dimensional micro-computed tomographic imaging of alveolar bone in experimental bone loss or repair. J Periodontol 78:273–281. https://doi.org/10.1902/jop.2007.060252.